

Mitochondrial absorption of blue light drives primate blue retinal cones into glycolysis

Jaimie Hoh Kam¹, Tobias W. Weinrich¹, Harpreet Sangha¹, Michael B. Powner², Robert
Fosbury^{1,3} and Glen Jeffery¹

¹University College London, Institute of Ophthalmology, ²City, University of London,
Centre for Applied Vision Research and ³European Southern Observatory, Munich,
Germany.

Correspondence to

Glen Jeffery

Institute of Ophthalmology

University College London

11-43 Bath St

London EC1V 9EL, UK

Phone +44 2076086837

Email g.jeffery@ucl.ac.uk

Photoreceptors have high energy demands and densely packed mitochondria through which light passes before phototransduction. Old world primates including humans have 3 cone photoreceptor types mediating colour vision with short (S blue), medium (M green) and long (L red) wavelength sensitivities¹. But S-cones are enigmatic. They comprise <10% of the total cone population and are not present in the human fovea², their responses saturate early³ and they are susceptible in ageing and disease⁴, especially diabetes⁵. Here we show that primate S-cones actually have few mitochondria and are fueled by glycolysis, not mitochondrial respiration. Glycolysis has a limited ability to sustain activity, explaining early S-cone saturation.

Mitochondria act as optical filters showing reduced light transmission at 400-450nm where S-cones are most sensitive (420nm). This absorbance is likely to arise in a mitochondrial porphyrin that absorbs strongly in the Soret band. Hence, reducing mitochondria will improve S-cone sensitivity but result in increased glycolysis as an alternative energy source, increasing diabetic vulnerability due to restricted glucose access. Further, glycolysis carries a price resulting in premature functional decline⁶ as seen in aged S-cones. Soret band absorption will also impact on mitochondrial rich M and L cones by reducing sensitivity at the lower end of their spectral sensitivity range resulting in increased differentiation from S-cone responses.

There is little of biological advantage in human/primate environments that is blue, and much in the eye that filters shorter wavelengths. Further, our S-cones are few and relatively frail. They are scarce in most mammals and some have lost them completely⁷. Their value, particularly to a progressively ageing population may be limited.

Photoreceptors have the greatest energy demand in the body, mediated by densely packed mitochondria in their inner segments (IS)⁸. Trichromatic vision in old world primates is achieved via signaling from three cone types with different spectral sensitivities: to blue (420nm), green (530nm) and red (560nm) light^{1,9}. However, relatively rare S-cones exhibit morphologically distinct IS¹⁰. Also, their psychophysical responses saturate early, similar to rod photoreceptors rather than other cones³. Although their number does not decline with age¹¹, they are functionally vulnerable⁵. We ask if these unique characteristics result from fundamental metabolic differences. Metabolic activity is driven by ATP generated either via mitochondrial respiration or glycolysis. The separate pathways can be identified by either pyruvate dehydrogenase to mark mitochondrial oxidative phosphorylation or lactate dehydrogenase marking glycolysis (Fig.1A). The mitochondrial route of production is more efficient while glycolysis provides rapid ATP delivery, but only briefly. However, glycolysis can be toxic⁶. We use these markers to determine which are employed by primate S-cones and if this differs from other cone types and why this should be.

Retinae from the old world primate *Macaca fascicularis* were immunostained for pyruvate or lactate dehydrogenase (PDH/LDH) and S-opsin. Pyruvate dehydrogenase complex has three enzymes E1, E2 and E3 converting pyruvate into acetyl-CoA. PDHE1 β is the rate limiting factor for the pyruvate dehydrogenase complex as it catalyses the reaction of PDHE2. Cones were distinguished morphologically by their clear cone shaped IS. Cones were positive for both PDHE1 β and PDHE2 with labelling confined to the mitochondrial containing IS. Staining for the two PDHE markers was very similar in cones across the retina. However, S-cones were consistently negative for both labels (Fig. 1B and C). All cones, irrespective of type, were LDH positive present throughout inner and outer segments (Fig. 1D). Hence, S-cones do not appear to employ mitochondria for ATP production but rely on glycolysis.

Mitochondria were revealed by staining with osmium and Sudan Black. Mitochondrial density was consistently lower in S-cones than other cone types. Fig. 2A shows an S-cone (arrow head) and adjacent, two non-S-cones. Also in S-cones, mitochondria never extended to the tip of the IS as found in other photoreceptors.

Sections were also stained for S-opsin and a voltage dependent anion channel marker (VDAC) present in outer mitochondrial membranes. VDAC mediates ATP and pyruvate transport across mitochondrial membranes and is linked with metabolic activity and regulates Ca^{2+} transport across the membrane¹². Fig. 2B shows VDAC label in red and the S-opsin in green. VDAC profiles are confined to outer IS regions reflecting patterns seen in Fig. 1B. However, in S-cones there is markedly reduced label. The area occupied by VDAC labelled profiles was measured in S-opsin cones and others. In S-opsin cells this was significantly lower ($P < 0.01$), being reduced by approximately 65% across the population (Fig. 2C). Reduced VDAC labelling in S-cones is consistent with the absence of pyruvate dehydrogenase in these cells (Fig. 1B and C). VDAC channels are also associated with the anti-apoptotic proteins Bcl2 and BclxL. These proteins maintain an open conformation of the channel. In doing so, they promote cell survival¹³. It is assumed that increased VDAC expression promotes cell death, while reduced expression is associated with cell survival¹². The reduced VDAC levels are consistent with S-cone survival with age in primates¹¹. Hence, S-opsin cones have relatively few mitochondria and do not express pyruvate dehydrogenase, which is a key marker of mitochondrial respiration.

If primate S-cones are fueled by glycolysis, is this a conserved feature of vertebrate photoreceptor function? Hence, we label both mouse and frog retinae for S-opsin and pyruvate or lactate dehydrogenase. Mice have only two cone types, S and combined M/L. They separate these with most

S-cones located in the ventral retina, and most M/L-cones in the dorsal retina¹⁴. In mouse, staining for pyruvate dehydrogenase was much greater in dorsal than ventral retina, consistent with the S-cone population being less reliant on mitochondrial function. Staining for lactate dehydrogenase was similar across the retina (Fig. 3A & B). Sections from frog (*Xenopus Laevis*) S-opsin cells were distributed throughout the retina. However, S-cones were mixed with some positive for pyruvate dehydrogenase and others negative (Fig. 3C). Again, staining for lactate dehydrogenase was relatively uniform. Hence, fueling of S-cone function may be different between mammals and amphibians.

As glycolytically fueled activity cannot be sustained, data from primates apparently explains why human S-cone psychophysical responses saturate early³. These data also explain selective S-cone functional decline in diabetes⁵, because here cells have restricted access to glucose on which glycolysis depends.

Glycolytic reliance is toxic due to production of methylglyoxal, termed “the dark side of glycolysis”. Methylglyoxal mediates glycation of proteins forming advanced glycation end products (AGEs) that increase endoplasmic reticulum stress driving neuronal degeneration and/or reduced function⁶. Such processes may underpin the selective early decline in aged human S-cone function. As primate S-cones are not lost with age¹¹, their functional decline is likely due to their distinct metabolism.

A driver for S-cone glycolysis is likely related to the reduced mitochondrial content in their IS. It had previously been noted by Curcio et al.¹⁰ that human S-cone IS were morphologically different from those of M- and L-cones. Given the very high packing density of mitochondria in M- and L-cones it is not surprising that reducing mitochondrial content by >60% influences their morphology. However, in

spite of this, Curcio et al.¹⁰ do not comment on the absence of mitochondria in the electron microscopic image of the S-cone IS compared with that of the M/L cone they present (their Fig. 3).

Why should S-cones have reduced mitochondrial density and employ glycolysis as their energy source? An explanation is suggested by the reverse orientation of photoreceptors in the vertebrate retina which demands that incoming light has to traverse the mitochondrion-rich IS before detection. Mitochondria have a marked drop in spectral transmittance at approximately 400–450nm that spans the peak S-cone sensitivity at 420nm^{8,15}. Bowmaker et al.¹⁵ noted the presence of a photostable pigment in the cones of the tree shrew, *Tupaia glis*, which might be associated with a porphyrin Soret band¹⁶. They show an absorbance spectrum with a peak at 418nm from a cone IS transverse spectral measurement yielding an absolute peak absorbance of 0.02. They also suggest that this could be associated with cytochrome c, part of the final stage of the electron transport chain in mitochondrial ATP production. This identification is supported by the extensive work on light-mitochondrion interactions by Karu and collaborators¹⁷.

Nakajima et al.⁸ measured the spectral absorbance of a known column density of suspended mitochondria extracted from guinea pig livers. Their transmission spectra showed a generally increasing extinction, extending into the blue, on which was superposed an absorption band with a width (FWHM) of about 45nm and centred at 418nm. This shows a close spectral similarity to the pigment measured by Bowmaker et al.¹⁸.

By isolating this band from the associated continuum extinction, we have scaled the Nakajima et al.⁸ absorbance result to the IS dimensions and mitochondrial content of primate cones. Note that the strength of the continuum extinction depends strongly on the redox state of the mitochondria while the band absorption remains constant. The result is expressed in Fig. 4, which shows the resulting effect on

the transmission of light in a longitudinal direction through the S- and the M/L- cones. We represent the IS as a cylinder with a diameter of 5 μ m and a length of 15 μ m, maximally filled with mitochondria representing the M/L-cones and a reduced population (by 65%) for the S-cones. Whilst only an estimate of the magnitude of the potential filtering effect: a loss of 35% in blue sensitivity for a full mitochondrial population and only 15% for the reduced population does provide a quantitatively feasible explanation for the special behavior of the S-cones.

If mitochondria spectrally filter it should be possible to identify psychophysical irregularities in spectral sensitivity curves of M- and L-cones in the region of the Soret band because of the high density of mitochondria in these cells. Both M- and L-cone sensitivity curves are asymmetric and have reduced sensitivity between 420–450nm that may be due to porphyrin filtering¹⁹. This would enhance discrimination between M/L- and S-cone sensitivities.

There is a wider evolutionary context to mitochondrial optical filtering in cone IS. In birds, reptiles and amphibians and some fish, the cone IS contains large oil droplets with different chromatic properties that act as lenses channeling and spectrally filtering light before absorption by outer segment opsins²⁰⁻²⁴. Mitochondria in front of the droplet may act to focus light onto the droplet surface²³. Droplets are absent in mammals with the exception of some marsupials where they are uncoloured²⁰. Our data indicate that the inner segment remains a region of optical filtering across many species and its presence in the light path provides one advantage in the transition from a compound eye to the inverted retina found in vertebrates. The price paid for reducing mitochondria is increased reliance on glycolysis with its inherent problems from an increased pace of ageing⁶. However, throughout the vast majority of human evolution, lifespan was probably <40 years, which is an age prior to significant human S cone decline⁴. Hence, adoption of glycolysis would have carried little cost. Only with recent expansion in Western lifespan do its damaging consequences become apparent.

Primate S-cones remain enigmatic. Our data explain some of their unique characteristics but not their evolution. Mammalian cones are different from those in birds, fish and amphibians and have been subject to different evolutionary drivers. The evolution of short wavelength vision in fish and amphibians was driven by the aquatic light environment where shorter wavelengths provide greater visual penetrance¹⁴. But a rationale for short wavelength sensitivity is harder to discern in mammals where there is little of significance in the environment that is blue. It is possible that, because of this, primates are losing their S-cones, which may explain their relatively low number here and in other mammals^{2,14}. A reason for this absence may be because chromatic aberration at shorter wavelengths will increase central retinal blur that may be important in human vision due to our attention to detail, particularly at short distances.

S-cones are labile compared to M- or L-cones that again mark them out as distinct. All cetaceans have lost their S-cones²⁵. While there is a rare human condition termed enhanced S-cone syndrome²⁶ where S-cone function is elevated and S-cone number may be >10 times greater than normal²⁷. During development, S-cones are the first to express opsin and many cells that subsequently express L- or M-opsin transiently express S-opsin²⁸. These features along with those described here mark S-cones out as distinct as and potentially more plastic than other photoreceptors.

Methods

Ocular tissues were acquired from *Macaca fascicularis* from an established colony under U.K. Home Office regulation and maintained by Public Health England. Eyes were retrieved at death following termination after sedation with ketamine and overdose of intravenous sodium pentobarbital. The primary purpose of animal usage was different from the aims of this study and eyes were only retrieved after death. The eyes were removed rapidly were fixed in 4% paraformaldehyde in 0.1M phosphate buffered saline (PBS) for several days and then transferred to phosphate buffer saline containing 0.025% sodium azide. Samples were taken from 5 young animals between 4-5 years and 5 old primates 14-15 years. Primates in this colony rarely lived beyond 18 years.

To determine if patterns of S-cone labeling in primates were conserved in other mammalian retinæ mice were also used in this study. Four month old C57 BL/6 were housed in standard conditions. These were sacrificed (N=4) by cervical dislocation and eye orientation marked by a small burn mark made to the dorsal aspect of the eye using a hot 18-gauge needle. The eyes were enucleated and fixed in 4% paraformaldehyde in PBS for 1 hour and cryoprotected in 30% sucrose overnight and embedded in OCT. 10 µm sections were cut and thaw-mounted onto charged slides. Slides were immunostained with a rabbit polyclonal anti-pyruvate dehydrogenase E2 from Abcam (ab66511, 1:200) and a goat polyclonal anti-OPN1SW (N-20) from Santa Cruz biotechnology, UK (sc-14363, 1:1000).

Immunohistochemistry. Primate eyes were fixed in 4% paraformaldehyde in PBS. After a few days, eyes were washed in PBS, dissected and the anterior tissues removed. A horizontal strip containing the retina, RPE and choroid was removed running from the temporal periphery, through the macular and fovea into the nasal retina. These were cryoprotected in 30% sucrose and then embedded in OCT (Optimal Cutting Temperature Tissue-Tek compound, leica). Frozen sections were cut at 10 µm and

immunostained with markers of mitochondrial metabolism with primary antibodies: Rabbit monoclonal anti-Lactate Dehydrogenase from Abcam, UK (ab134187, 1:200); Mouse monoclonal anti-Pyruvate Dehydrogenase E1 β subunit from Abcam, UK (ab110331, 1:200); a rabbit polyclonal anti-pyruvate dehydrogenase E2 from Novus biologicals (NBP2-34065), a goat polyclonal anti OPN1SW (N-20 from Santa Cruz Biotechnology, UK) (sc-14363, 1:1000). A rabbit polyclonal voltage dependent anion channel 1 marker from Novartis Biologicals (NBP1-45921). Secondary antibodies in the double labelling experiment were fluorescent conjugate Alexa Fluor 568 (1:2000, Invitrogen, UK) or 488 (1:2000, Invitrogen, UK). The nuclei were counterstained with a nuclear marker 4', 6-diamino-2-phenylindole (DAPI) (Sigma-Aldrich, UK). Slides were mounted in Vectashield (Vector Laboratories, UK) and coverslipped. Sections were viewed and images captured using an Epi-fluorescence and bright-field microscope (Olympus BX50F4, Olympus, UK) and a Nikon DXM1200 (Nikon, UK) digital camera.

Resin embedded histology. 5 eyes from young and 5 eyes from old primates were dissected and a horizontal strip of the neural retina was removed running from the periphery through the centre was used as flatmount and processed for immunohistochemistry. After several PBS washes, the retinal tissues were blocked and permeabilised with 5% Normal Donkey serum in 3% (v/v) Triton X-100 in PBS for 2h. Samples were incubated overnight in a goat polyclonal antibody to OPN1SW (N-20 from Santa Cruz Biotechnology, UK) (sc-14363, 1:1000) made in 1% Normal Donkey Serum in 3% Triton X-100 in 0.1M PBS. After primary antibody incubation, samples were washed repeatedly in PBS and incubated in a biotinylated anti goat secondary antibody for 2 hours at room temperature. After the secondary antibody incubation, the flatmounts were washed several times and incubated in a ready to use horseradish peroxidase Streptavidin solution (VECTOR Laboratories, UK) for 30 minutes, followed by a peroxidase substrate solution, 3,3-diaminobenzidine (DAB) for 5 minutes. The

flatmounts were afterwards processed for resin embedded plastic and were therefore fixed with 2% paraformaldehyde and 2% glutaldehyde in PBS for 24h, followed by repeated PBS washing and then were post fixed in 1% OsO₄ in 0.1M PBS for 2h. They were then thoroughly washed in distilled water and dehydrated through a graded series of ethanol. Then infiltrated, polymerised and embedded in Technovit 7100 historesin (Taab Laboratories equipment, UK). Resin sections were cut at 2.5µm, histologically stained with Sudan Black B and mounted in Depex and coverslipped.

Statistical analysis. For comparison between the two groups, a Mann-Whitney U test was used. Data were analysed using GraphPad Prism version 5.0 for windows (GraphPad, San Diego, USA).

Mitochondrial absorption modeling. Measurements of the optical absorbance of a suspension of mitochondria taken from guinea pig livers were extracted from the transmittance data shown in Fig. 3 of Nakajima et al.⁸ After measuring their 'Reduction' and 'Oxidation' transmission curves, central absorbance values and bandwidths (FWHM) were derived for the selective absorption curves centred at 418nm by interpolating a continuum across the band from both their reduced and oxidised measurements. This results in central absorbance values for the band alone of 0.061 and 0.055 respectively, yielding an average of 0.06 with an estimated error of ~0.01. This calculation assumes the difference between the reduced and oxidized Nakajuma et al.⁸ transmission curves is entirely due to the continuous extinction and not to the Soret band absorption.

This average value was then scaled for the ratios of transmission pathlength and of the mitochondrial volume density values from the Nakajuma et al.⁸ experiment and a schematic cone inner segment model consisting of a cylinder of diameter d µm and length l µm.

To produce Figure 4, we assumed $d = 5$ and $l = 15$ and that the IS of M/L-cones have a mitochondrial filling factor of unity for the M/L cones and 0.35 for the S cone. The transmission curves are then calculated using a Lorentzian absorbance profile having a FWHM of 45nm.

References

1. Knowles, A., Davson, H. & Dartnall, H.J.A. *The Photobiology of Vision*, (Academic Press, 1977).
2. Calkins, D.J. Seeing with S cones. *Prog Retin Eye Res* **20**, 255-287 (2001).
3. Mollon, J.D. & Polden, P.G. Saturation of a retinal cone mechanism. *Nature* **265**, 243-246 (1977).
4. Werner, J.S. The Verriest Lecture: Short-wave-sensitive cone pathways across the life span. *J Opt Soc Am A Opt Image Sci Vis* **33**, A104-122 (2016).
5. Greenstein, V.C., Hood, D.C., Ritch, R., Steinberger, D. & Carr, R.E. S (blue) cone pathway vulnerability in retinitis pigmentosa, diabetes and glaucoma. *Invest Ophthalmol Vis Sci* **30**, 1732-1737 (1989).
6. Xing, Y., *et al.* Injury of cortical neurons is caused by the advanced glycation end products-mediated pathway. *Neural Regen Res* **8**, 909-915 (2013).
7. Hunt, D.M. & Peichl, L. S cones: Evolution, retinal distribution, development, and spectral sensitivity. *Vis Neurosci* **31**, 115-138 (2014).
8. Nakajima, Y., *et al.* Molecular characterization of a novel retinal metabotropic glutamate receptor mGluR6 with a high agonist selectivity for L-2-amino-4-phosphonobutyrate. *J Biol Chem* **268**, 11868-11873 (1993).
9. Mollon, J.D. Color vision. *Annu Rev Psychol* **33**, 41-85 (1982).
10. Curcio, C.A., *et al.* Distribution and morphology of human cone photoreceptors stained with anti-blue opsin. *J Comp Neurol* **312**, 610-624 (1991).
11. Weinrich, T.W., *et al.* No evidence for loss of short-wavelength sensitive cone photoreceptors in normal ageing of the primate retina. *Sci Rep* **7**, 46346 (2017).

12. Dubey, A.K., Godbole, A. & Mathew, M.K. Regulation of VDAC trafficking modulates cell death. *Cell Death Discov* **2**, 16085 (2016).
13. Gottlob, K., *et al.* Inhibition of early apoptotic events by Akt/PKB is dependent on the first committed step of glycolysis and mitochondrial hexokinase. *Genes Dev* **15**, 1406-1418 (2001).
14. Bowmaker, J.K. Evolution of vertebrate visual pigments. *Vision Res* **48**, 2022-2041 (2008).
15. Bowmaker, J.K., Astell, S., Hunt, D.M. & Mollon, J.D. Photosensitive and photostable pigments in the retinæ of Old World monkeys. *J Exp Biol* **156**, 1-19 (1991).
16. Brunet, C., Antoine, R., Lemoine, J. & Dugourd, P. Soret Band of the Gas-Phase Ferri-Cytochrome c. *J Phys Chem Lett* **3**, 698-702 (2012).
17. Karu, T. Primary and secondary mechanisms of action of visible to near-IR radiation on cells. *J Photochem Photobiol B* **49**, 1-17 (1999).
18. Bowmaker, J.K., Kovach, J.K., Whitmore, A.V. & Loew, E.R. Visual pigments and oil droplets in genetically manipulated and carotenoid deprived quail: a microspectrophotometric study. *Vision Res* **33**, 571-578 (1993).
19. Stockman, A. & Sharpe, L.T. Human cone spectral sensitivities: a progress report. *Vision Res* **38**, 3193-3206 (1998).
20. Walls, G.L. *The vertebrate eye and its adaptive radiation*, (Hafner Publishing Company New York, 1942).
21. Stavenga, D.G. & Wilts, B.D. Oil droplets of bird eyes: microlenses acting as spectral filters. *Philos Trans R Soc Lond B Biol Sci* **369**, 20130041 (2014).
22. Vorobyev, M. Coloured oil droplets enhance colour discrimination. *Proc Biol Sci* **270**, 1255-1261 (2003).
23. Wilby, D. & Roberts, N.W. Optical influence of oil droplets on cone photoreceptor sensitivity. *J Exp Biol* **220**, 1997-2004 (2017).

24. Kram, Y.A., Mantey, S. & Corbo, J.C. Avian cone photoreceptors tile the retina as five independent, self-organizing mosaics. *PloS one* **5**, e8992 (2010).
25. Peichl, L., Behrmann, G. & Kroger, R.H. For whales and seals the ocean is not blue: a visual pigment loss in marine mammals. *Eur J Neurosci* **13**, 1520-1528 (2001).
26. Haider, N.B., *et al.* Mutation of a nuclear receptor gene, NR2E3, causes enhanced S cone syndrome, a disorder of retinal cell fate. *Nat Genet* **24**, 127-131 (2000).
27. Ripamonti, C., *et al.* Vision in observers with enhanced S-cone syndrome: an excess of s-cones but connected mainly to conventional s-cone pathways. *Invest Ophthalmol Vis Sci* **55**, 963-976 (2014).
28. Cornish, E.E., Xiao, M., Yang, Z., Provis, J.M. & Hendrickson, A.E. The role of opsin expression and apoptosis in determination of cone types in human retina. *Exp Eye Res* **78**, 1143-1154 (2004).
29. Dartnall, H.J., Bowmaker, J.K. & Mollon, J.D. Human visual pigments: microspectrophotometric results from the eyes of seven persons. *Proc R Soc Lond B Biol Sci* **220**, 115-130 (1983).

Acknowledgments. The research was funded by the BBSRC (BB/N000250/1). We thank Public Health England for the supply of tissue used in this study and S. Holmes for her technical assistance.

Author contributions. JHK, TWW and GJ conceived of the experiment. Experiments were performed by, JHK, TWW, MBP, HS and RF. Data analysis was undertaken by JHK, TWW, HS, and RF. All authors wrote and revised the manuscript.

Author information. Reprints and permissions, information is available at www.nature.com/reprints.

All authors declare that they have no competing interest. Correspondence and requests for materials should be addressed to g.jeffery@ucl.ac.uk

Figures

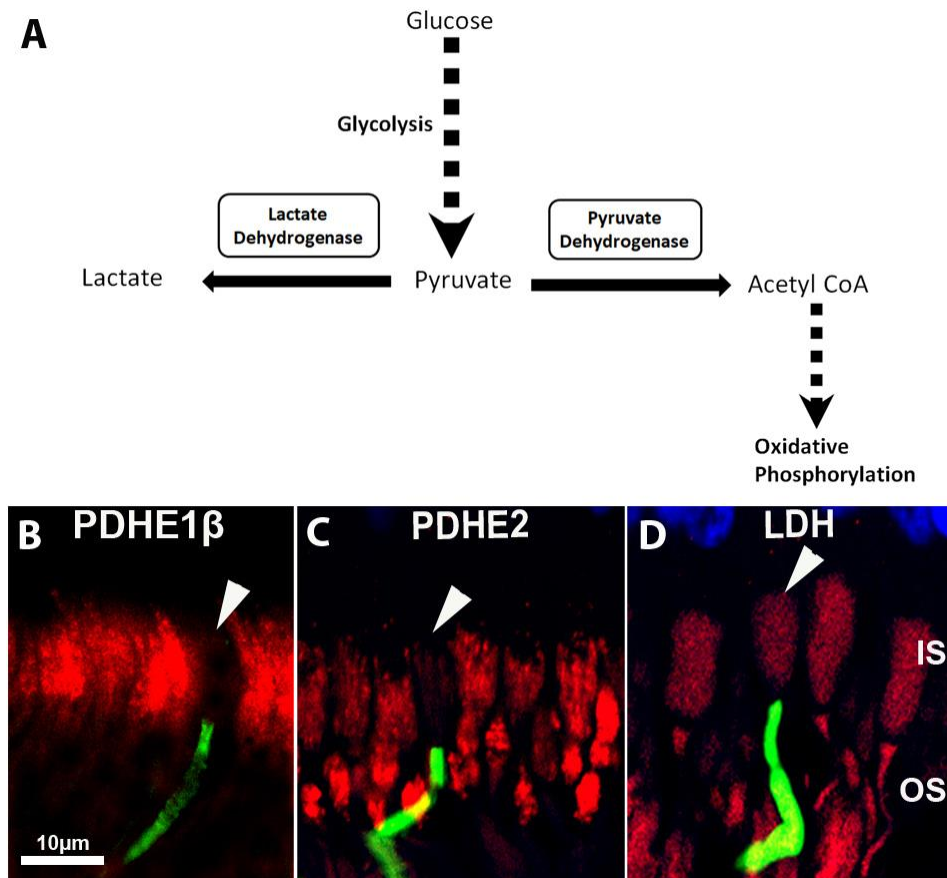


Figure 1. **A.** Schematic representation of pathways for ATP production via either pyruvate dehydrogenase leading to mitochondrial oxidative phosphorylation or via lactate dehydrogenase as part of glycolysis. **B-D.** We use pyruvate dehydrogenase (PDH) and lactate dehydrogenase (LDH) markers to define these pathways labelling central primate retina. Labelling for PDH is subdivided into PDHE1 β (**B**) and PDHE2 (**C**). PDHE1 β is the rate limiting factor for the pyruvate dehydrogenase complex as it catalyses the reaction of PDHE2. PDH is in red in **B** and **C**. S-cones are labeled in green

and marked with a white arrow head. PDH label is confined to mitochondrial containing inner segments (IS). However, the S-cones are negative for both PDH forms. D is stained for LDH. Here label is present in inner (IS) and outer segments (OS). All photoreceptors, including S-cones are LDH positive. Blue staining to the top is the outer nuclear layer.

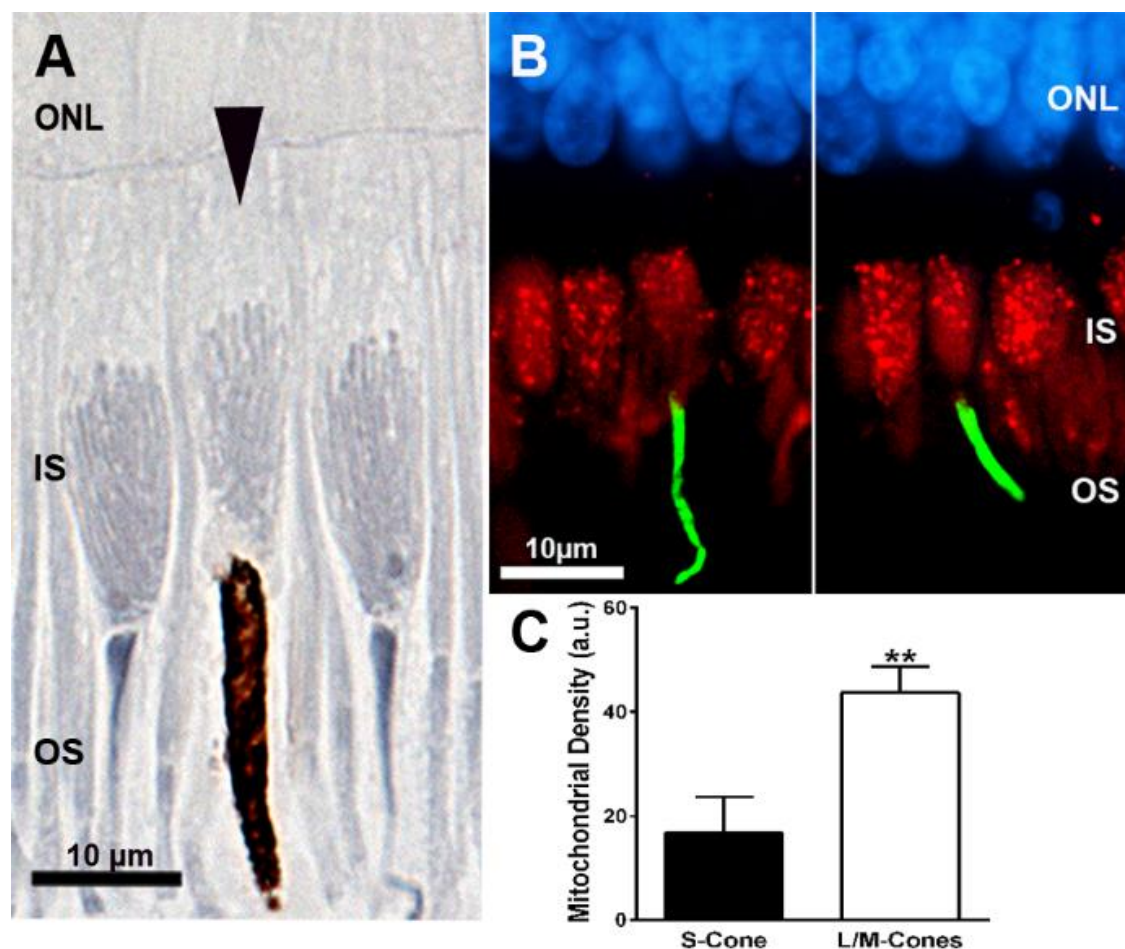


Figure 2. Cone inner segments (IS) where mitochondria have been labelled with two separate methods along with S-opsin. A. Sections stained with osmium and Sudan Black. Here mitochondria are seen as elongated structures within the IS oriented towards the OS. The central cone marked with an arrow head has an S-opsin positive OS. In this cell mitochondrial density is relatively low and mitochondria do not extend fully to the OS. B. Two images from the central retina stained with a voltage dependent

anion channel (VDAC) present in mitochondria (red) and S-opsin (green). Photoreceptor nuclei in the outer nuclear layer (ONL) are stained in blue. C. The area of VDAC label in the cones has been measured in S-opsin positive and S-opsin negative cells. There is >60% significant reduction in the area occupied by VDAC label in S-cones compared to other cone types.

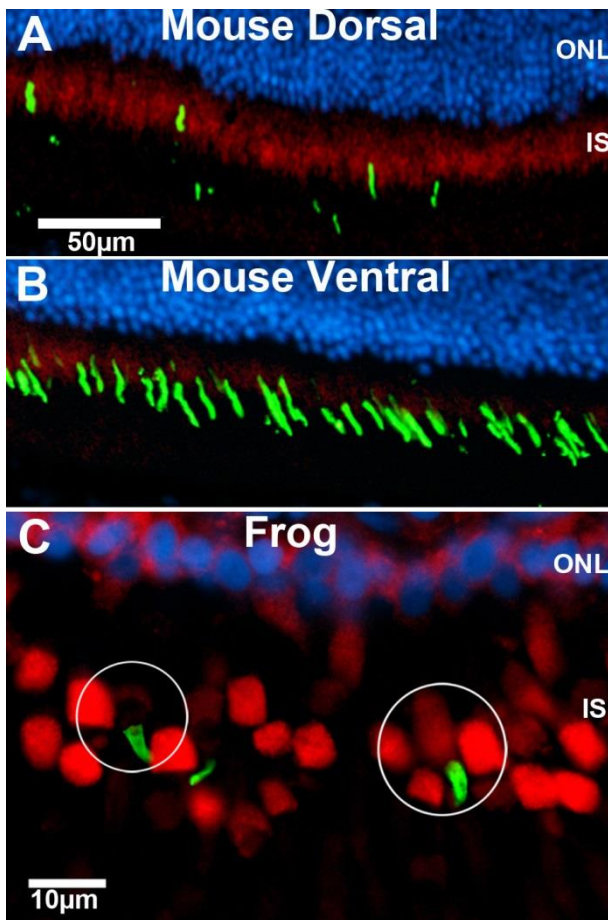


Figure 3. Staining for pyruvate dehydrogenase (red) and S-opsin (green) in mouse (upper panels) and frog (lower panel). In rodents S-cones are largely confined ventrally. In this region of the retina there was much less pyruvate dehydrogenase than in dorsal regions consistent with the notion that these cones may not be using mitochondrial respiration similar to primates. However, in frogs S-cones were identified that were both positive and negative for pyruvate dehydrogenase. An example of each is circled.

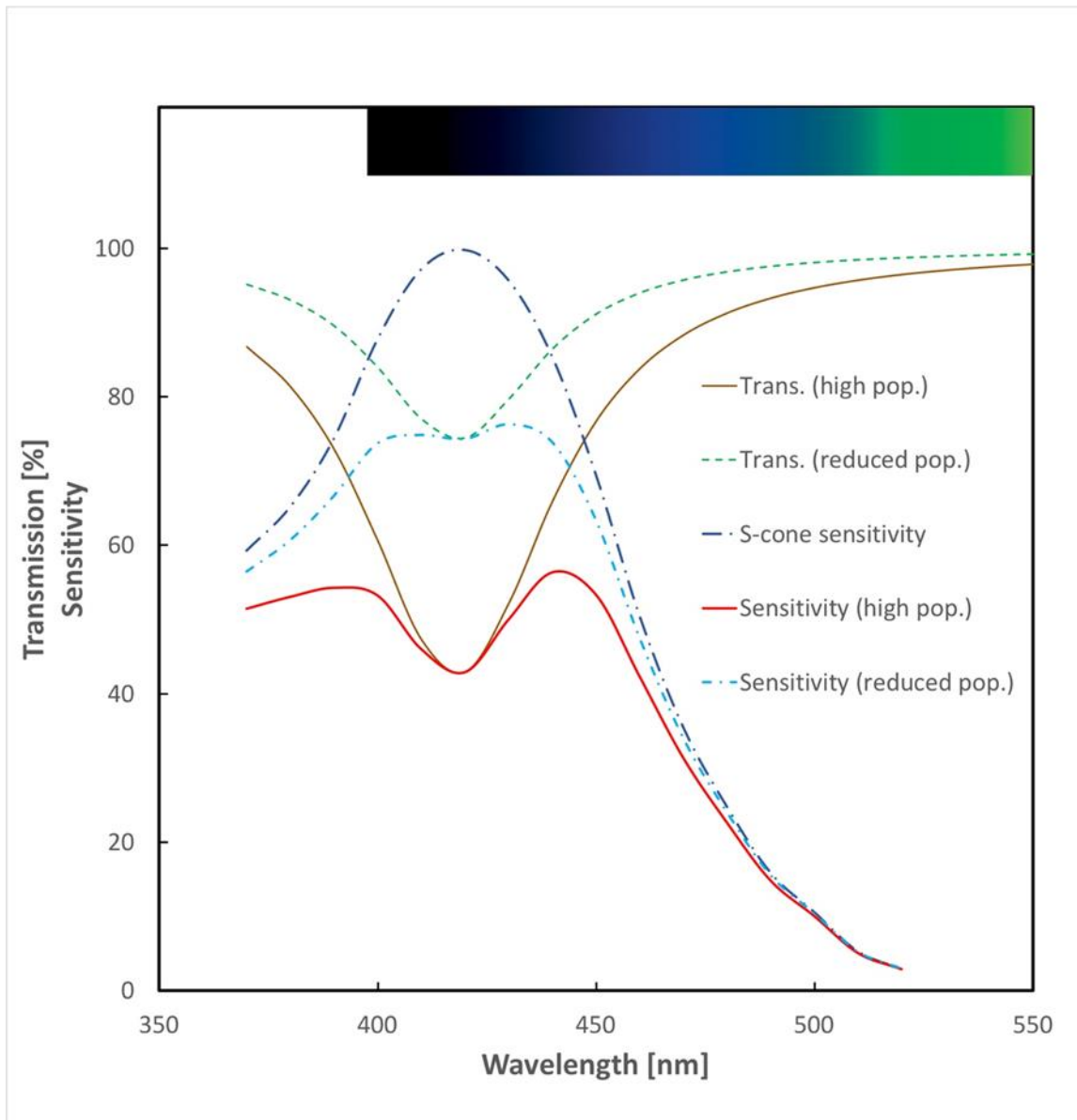


Figure 4 Schematic representation of the effect on S-cone response to Soret band absorption by the population of mitochondria in the inner segment of the cell. This is based on our scaling of the mitochondrial absorbance measured by Nakajima et al.⁸ and our own estimates of mitochondrial numbers in primate S- and M/L-cones. The solid lines (brown and red) show the response as it would be if the S-cones had the same high complement of mitochondria seen in the M- and L-cones. The dashed lines (green and blue) show the higher response resulting from the reduced mitochondrial number seen in the S-cone cells. Integrals (between 370 and 470nm) of the absorbed Dartnall et al.²⁹ S-

cone sensitivity curve with these two populations show a sensitivity loss of 35% with the high M/L cone population which is reduced to 15% loss with the reduced S-cone numbers.